We are IntechOpen, the world's leading publisher of Open Access books Built by scientists, for scientists

6,900
Open access books available

185,000
International authors and editors

200M
Downloads

Our authors are among the

154
Countries delivered to

TOP 1%
most cited scientists

12.2%
Contributors from top 500 universities



WEB OF SCIENCE™

Selection of our books indexed in the Book Citation Index in Web of Science™ Core Collection (BKCI)

Interested in publishing with us?
Contact book.department@intechopen.com

Numbers displayed above are based on latest data collected.
For more information visit www.intechopen.com



Chapter

Cathode for Thin-Film Lithium-Ion Batteries

Yuan-Li Ding

Abstract

Thin-film lithium-ion batteries (LIBs) have attracted considerable attention for energy storage device application owing to their high specific energy compared to conventional LIBs. However, the significant breakthroughs of electrochemical performance for electrode materials, electrolyte, and electrode/electrolyte interface are still highly desirable. This chapter firstly gives an overview of cathode materials including lithium-containing cathode (e.g., $LiCoO_2$, $LiMn_2O_4$, $LiFePO_4$, $LiNi_{1-x-y}Mn_xCo_yO_2$, $LiNi_{0.5}Mn_{1.5}O_4$) and lithium-free cathode (e.g., vanadium oxides) for LIBs in terms of specific capacity, energy density, working voltage, cycling life, and safety. In the meanwhile, the existing drawbacks and limitations of various battery chemistries are also analyzed. Furthermore, some modification strategies for these cathode materials have also been discussed for improving electrochemical performance. Finally, the thin-film Li-ion battery applications of these cathode materials are summed up toward next-generation flexible and high-energy devices.

Keywords: cathode, nanotechnology, energy density, thin-film lithium-ion batteries

1. Overview of cathode materials

Since lithium-ion batteries (LIBs) gained the commercial success in 1991 [1], they have received considerable attention in various areas including consumer electronics, power tools, electric vehicles, and grid energy storage owing to their high energy density, low cost, long cycle life, and environmentally benignity. The energy density of LIBs in 1991 is only 80 Wh kg^{-1} at a cell level and has been currently increased to 200–250 Wh kg^{-1} (at a cell level). The main reason is attributed to the significant improvement of battery materials and battery technology. Especially for cathode materials, they dominate the whole cell performance compared to graphite anode.

Up to now, various cathode materials have been proposed and developed such as layered structure $LiCoO_2$, $LiMnO_2$, $LiNiO_2$, ternary $LiNi_{1-x-y}Mn_xCo_yO_2$, spinel $LiMn_2O_4$ (LMO), spinel $LiNi_{0.5}Mn_{1.5}O_4$ (LNMO), and polyanion-based cathode including $LiFePO_4$ and $Li_3V_2(PO_4)_3$ [2], as shown in **Figure 1**. Typically, transition metals of such cathode materials undergo an oxidation process to higher oxidation state when Li^+ ions are removed. While oxidation of the transition metals can retain charge neutrality in the compound, Li^+ removal/insertion usually causes phase changes and structural strain. In this regard, cathode materials that are stable enough over a wide composition range must be employed. Thus, the structural stability of cathode materials is a key during Li^+ extraction/insertion processes. As for discharge process, Li^+ ions are reinserted into the cathode materials and electrons from anode reduce transition metal ions in the cathode to a lower valence. The rates

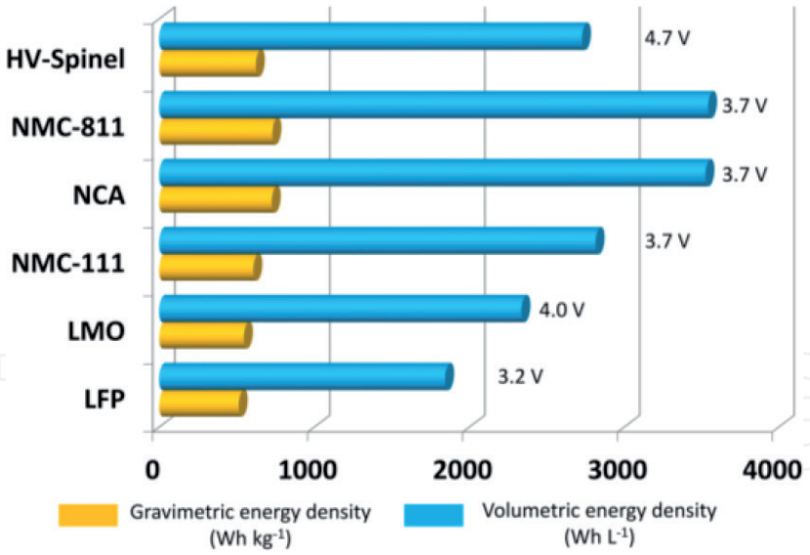


Figure 1.
Gravimetric and volumetric energy densities of various cathode materials at a material level. LFP, $LiFePO_4$; LMO, $LiMn_2O_4$; NMC-111, $LiNi_{1/3}Mn_{1/3}Co_{1/3}O_2$; NCA, $LiNi_{0.8}Co_{0.15}Al_{0.05}O_2$; NMC-811, $LiNi_{0.8}Mn_{0.1}Co_{0.1}O_2$; HV-spinel, $LiNi_{0.5}Mn_{1.5}O_4$.

of the two processes, as well as access of Li^+ ions in the electrolyte to electrode surface, dominate the maximum discharge current. Therefore, cathode performance depends critically on the microstructure and morphology of electrode as well as the intrinsic electrochemical properties of the cathode materials. For instance, much effort has been currently focused on the development of nanosized electrode materials for shortening Li^+/electron transport length and increasing contact areas of electrode/electrolyte interface. This chapter will mainly discuss cathode materials for LIBs and their potential applications for thin-film Li-ion microbatteries.

2. Layered transition metal oxide cathode

Layered transition metal oxides are the most commonly used cathode materials for LIBs such as $LiCoO_2$, $LiNiO_2$, $LiMnO_2$, and $LiTiS_2$. Such cathode materials have typical layered structure, as illustrated in **Figure 2**. $LiCoO_2$ is relatively one of the most mature cathode materials, which will be discussed in the following section. However, the crystal structure of Li_xCoO_2 becomes unstable when Li^+ extracts beyond $x > 0.5$, leading to oxygen release [3]. Considering the shortcomings and costly Co resource of $LiCoO_2$, layered ternary transition metal oxides $LiNi_{1-x-y}Mn_xCo_yO_2$ (NMC) have been widely investigated and developed in recent years.

2.1 $LiCoO_2$

As one of the typical intercalation compound families, $LiCoO_2$ was first reported and studied by John B. Goodenough in 1980 for LIBs [4]. It has an a-$NaFeO_2$ structure containing only one kind of cation in the transition meta layer. $LiCoO_2$ is widely used as cathode materials for LIBs, especially for portable electronics. Although $LiCoO_2$ is the most widely used cathode materials for LIBs, the practical capacity available is only around 140 mAh g^{-1}, half of the theoretical capacity (ca. 280 mAh g^{-1}). It corresponds to the 50% Li removal from $LiCoO_2$ because further lithium extraction from $LiCoO_2$ usually induces the structural transition from hexagonal to monoclinic phase and Co dissolution at the highly oxidized state, thus leading to rapid capacity decay. To enhance the capacity retention of $LiCoO_2$ at the

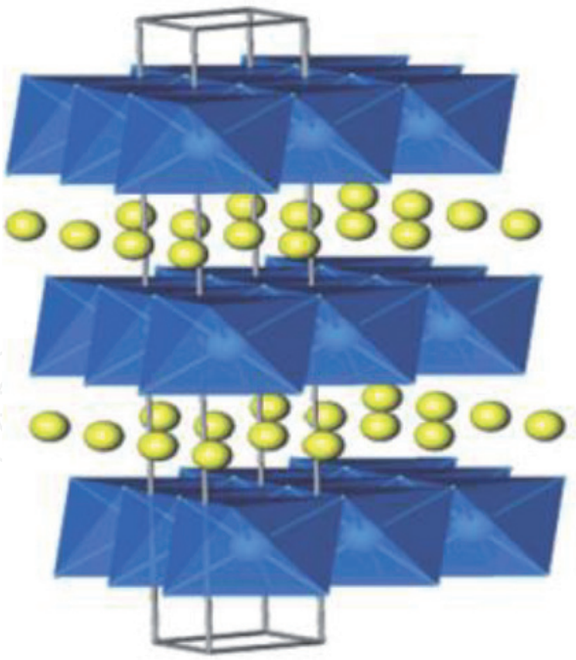


Figure 2.
Layered structure of $LiMO_2$ (M = Ni, Co, Mn), showing the lithium ions between the transition metal oxides.

higher cutoff potential (4.4–4.5 V), surface modifications (e.g., surface coating) on the $LiCoO_2$ surface have been employed since such the strategies can effectively restrict the lattice constant change and the transition of hexagonal to monoclinic phase change upon cycling. The mechanism of such capacity improvement for $LiCoO_2$ was not widely identified. Dahn group found that the poor capacity retention of $LiCoO_2$ at the high delithiation potential (4.5 V) was attributed to the growth of impedance at the $LiCoO_2$ surface caused by side reactions [5]. As for $LiCoO_2$, although a higher reversible capacity by using a higher cutoff potential can be obtained, such a cathode still faces a thermal stability concern, resulting in a safety issue. Moreover, Co in the delithiated $Li_{1-x}CoO_2$ possesses high oxidizing power and easily induces the more side reactions with organic electrolytes. Thus, $LiCoO_2$ is mainly used as low-power devices such as consumer electronics.

2.2 $LiNi_{1-x-y}Mn_xCo_yO_2$

Although $LiCoO_2$ exhibits the most early commercial success, the intrinsic structural stability upon delithiation and high raw material cost of $LiCoO_2$ have pushed the development of a new class cathode materials. As an alternative cathode, layered structured Li_xNiO_2 has been developed owing to its relatively low cost and high working potential [6]. However, pristine Li_xNiO_2 is not a promising cathode candidate because of its some drawbacks. For example, more than 200 mAh g^{-1} can be obtained from stoichiometric $LiNiO_2$ at a relatively high voltage (4.5 V vs. Li/Li^+). Moreover, a 20% capacity loss occurs in the first cycle owing to the structural modification when charged below x = 0.5. Besides electrochemical properties, stoichiometric $LiNiO_2$ with a Li/Ni ratio of 1:1 is still difficult to be synthesized because of the cation mixing of Ni^{2+} and Ni^{3+} owing to the similarity of ionic radii of Li^+ (0.76 Å) and Ni^{2+} (0.69 Å) [7]. Moreover, Li_xNiO_2 is usually Li-deficient because it is difficult to prepare stoichiometric $LiNiO_2$. To address this issue, the synthesis condition usually needs oxygen instead of air atmosphere and a slight excess of $LiNO_3$.

Considering the advantages and shortcomings of $LiNiO_2$, metal-doped $LiNiO_2$, especially ternary layered cathode NMC and $LiNi_{0.8}Co_{0.15}Al_{0.05}O_2$ (NCA), has recently

attracted considerable attention because it shows good structural stability, higher specific capacity up to 220 mAh g^{-1}, higher energy density, and relatively simple synthesis [8]. By introducing Mn and Co or Al and Co into $LiNiO_2$, the cation mixing of Ni^{2+}/Ni^{3+} can be effectively restricted. In the meanwhile, $LiNi_{1-x-y}Mn_xCo_yO_2$ can be synthesized in the air without the necessity to use pure oxygen atmosphere. As for NMC cathode, $LiNi_{1/3}Mn_{1/3}Co_{1/3}O_2$ (NMC-111) is currently the most common form of NMC cathode materials and is widely employed in LIBs [9]. To further enhance energy density and reduce cost, increasing Ni content and lowering Co content in NMC cathode are effective solutions such as $LiNi_{0.5}Mn_{0.3}Co_{0.2}O_2$ (NMC-532), $LiNi_{0.6}Mn_{0.2}Co_{0.2}O_2$ (NMC-622), and $LiNi_{0.8}Mn_{0.1}Co_{0.1}O_2$ (NMC-811), as shown in **Figure 3**.

It is well known that Ni is beneficial for achieving high energy density but poor stability, especially at the charged state. Mn will induce the formation of a spinel structure to realize a low internal resistance but results in a low energy density. Compared to Ni and Mn, Co has the limited resources (Co reserve available is around 7.1 million tons) [10], high price, and high toxicity. Thus, NMC battery chemistry will gradually lessen the use of Co element and simultaneously employ high Ni and low Mn for realizing the best electrochemical performance by combining the respective merits of Ni, Mn, and Co. NMC-111, NMC-442, and NMC-532 are currently the state of the art of cathode materials. In the very recently, Ni-rich NMC cathodes including NMC-622 and NMC-811 have been widely investigated and will be adopted in the LIBs owing to their higher energy density and lower cost. This is very favorable for automotive applications. On the other hand, Mn^{3+} has the lowest octahedral site stabilization energy (OSSE) and tends to migrate, resulting in a layered-to-spinel transition upon lithiation/delithiation process. In contrast, Co^{3+} has the highest OSSE and exhibits excellent structural stability, but it suffers from poor chemical stability during lithium extraction over 50%, which is attributed to an overlap of the t_{2g} band of low-spin $Co^{3+/4+}$ with the top of the 2p band of O^{2-} [11], as shown in **Figure 3b**. Compared to Co, Mn provides better chemical stability because $Mn^{3+/4+}$ e_g band is further above the top of the 2p band of the O^{2-}. Compared to Co and Mn, Ni shows a moderate structural and chemical stability considering that it has a higher OSSE than Mn^{3+}, and the e_g band of low-spin $Ni^{3+/4+}$ just touches the top of the O^{2-} 2p band. Thus, developing Co-less and Ni-rich NMC cathode will be very desirable.

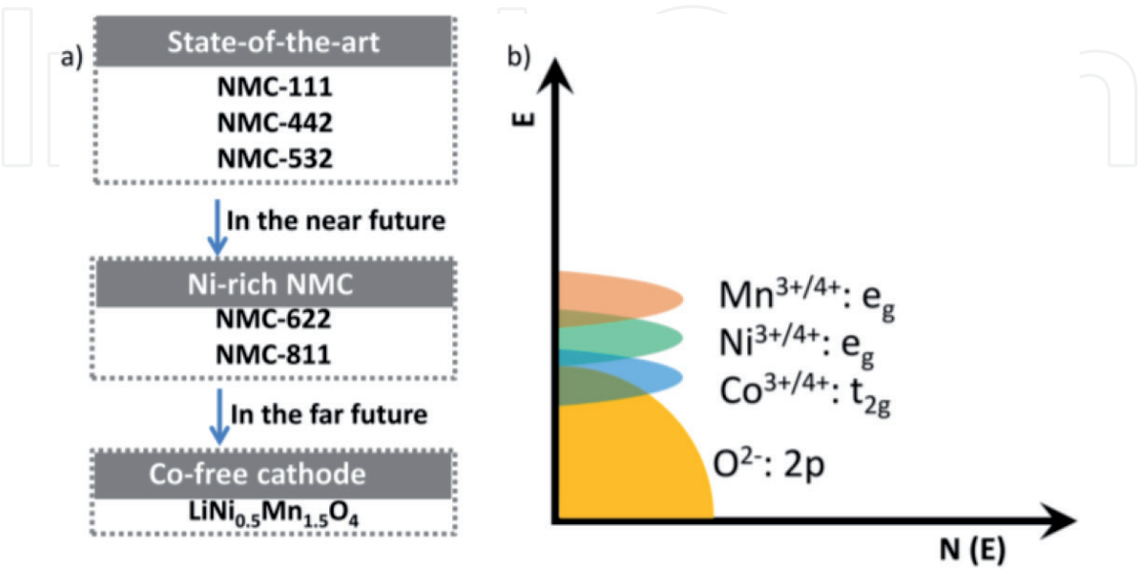


Figure 3.
(a) The state-of-the-art NMC cathode materials, near-future NMC materials, and far-future cathode materials. (b) Schematic diagram of the positions of the various redox couples relative to the top of the oxygen: 2p band.

The commercial success of NMC-111 facilitates the development of other NMC materials by combining the individual advantages of Ni, Mn, and Co in the layered crystal structure with varying concentration to realize high capacity and high energy density. As discussed previously, a high Ni content is favorable to achieve a high reversible capacity. On the other hand, the introduction of Mn can enhance the structural and thermal stability at the deeply delithiated state, while Co dopant in NMC can improve the layered ordering as well as rate performance and specific capacity owing to its redox activity. Sun et al. have systematically investigated the effect of chemical compositions for the ternary NMC materials on reversible capacity, cyclability, and thermal stability [12], as displayed in **Figure 4**. The NMC materials with higher Ni content show higher reversible capacities, but it shows a decreased capacity retention at both 25 and 55°C. In addition, the exothermic reaction for Ni-rich NMC usually occurs at a lower temperature with a larger heat generation upon charging to 4.3 V vs. Li/Li^+, which is a good agreement with the phenomena of capacity retention decrease with increasing Ni content (**Figure 4**). Such findings confirm that Ni-rich NMC possesses a higher specific capacity but poor thermal stability and capacity retention upon cycling, as shown in **Figure 4**. To address this problem, a novel material design by tuning chemical composition in the core and shell has been proposed by Sun group [13]. The first generation is a core-shelled structure based on Ni-rich NMC-811 as core and Mn-rich $LiNi_{0.5}Mn_{0.5}O_2$ as shell (**Figure 5a**). The core can offer high capacity, while the shell guarantees the surface stability. Such structural design, however, also has some drawbacks. For example, boundary cracks between active particles often formed owing to different

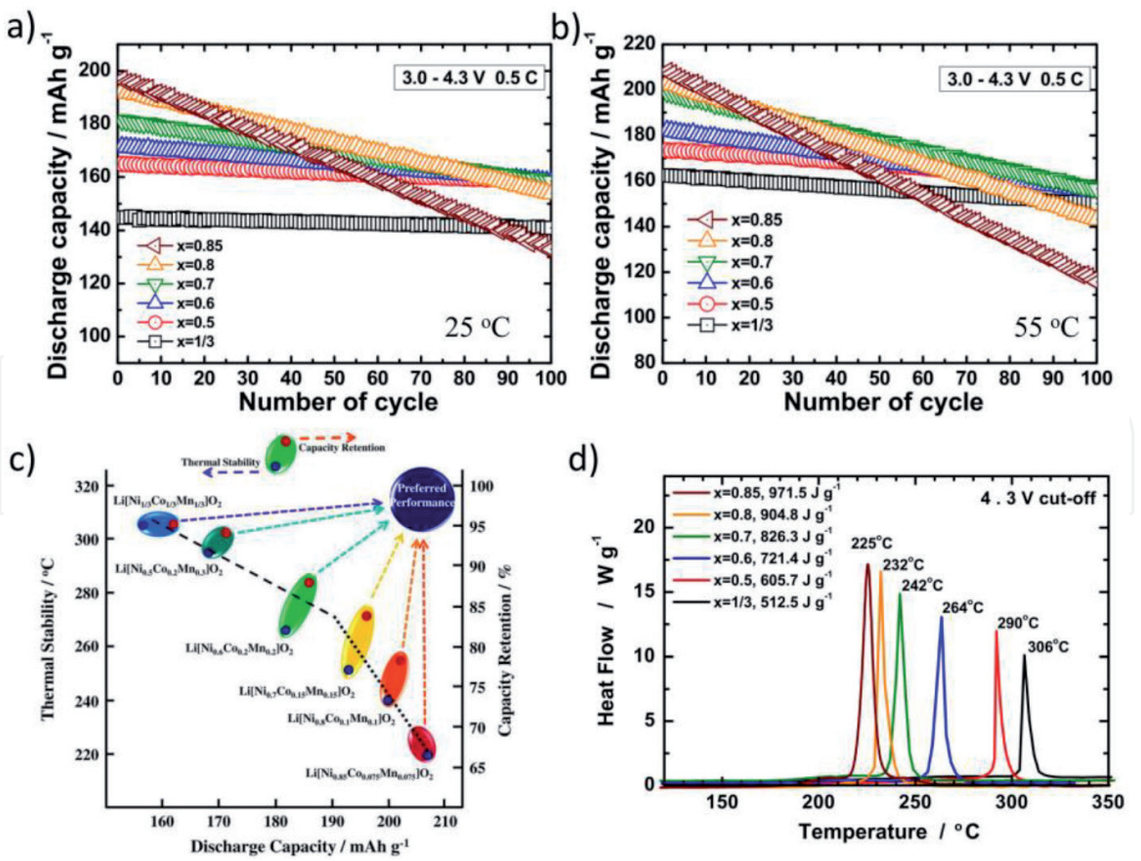


Figure 4.
Discharge capacity as a function of cycle number for various LiNixMnyCozO2 (x = 1/3, 0.5, 0.6, 0.7, 0.8, and 0.85) cathodes at (a) 25°C and (b) 55°C. The current density is 100 mA g^{-1} (0.5 C) in the voltage range of 3.0–4.3 V [12]. (c) The map of relationship between discharge capacity and thermal stability and capacity retention for $LiNi_xMn_yCo_zO_2$ (x = 1/3, 0.5, 0.6, 0.7, 0.8, and 0.85) cathode. (d) DSC curves of the above NMC cathode materials.

volume changes between the core and the shell structures upon cycling tend to induce the formation of boundary cracks, leading to major mechanical fracture of active particles and capacity decay. Thus, another core-shelled gradient-type and full concentration gradient-type NMC materials have been proposed and developed [14], as illustrated in **Figure 5b**. This unique design minimizes the propagation of boundary cracks and is beneficial to enhancing cycling stability.

2.3 Layered NCA cathode

Similar to NMC-811 cathode, $LiNi_{0.8}Co_{0.15}Al_{0.05}$ (NCA) is also a Ni-rich cathode, showing a relatively high energy density and low cost. The introduction of element Al in NCA can minimize the detrimental phase transition and improve the thermal behavior of the cathode. Al is a favorable dopant in a specific capacity because of its lower atomic weight than the other transition metal elements. Thus, Al-doped $LiNiO_2$ shows an increased specific capacity. Moreover, the presence of Al^{3+} in the transition metal layer tends to reduce the a-axis but increase the c-axis parameters because of α-$LiAlO_2$ (a = 2.8 Å and c = 14.23 Å), which decrease the cationic disorder in the Li layer. It is similar to the effect of Co^{3+}. However, a large amount of Al doping would lead to the reduction of specific capacity because Al is electrochemically inactive. On the other hand, Al^{3+} can effectively enhance the working voltage owing to the weakening of the Ni-O bond by the stronger Al-O bond through the inductive effect. Thus, a reasonable balance between reduced capacity and increased working voltage should be considered for designing high-performance Al-doped $LiNiO_2$. It is acknowledged that Al doping (5 atom%) and Co doping (15 atom%) is the optimized results [11]. In recent years, double metal doping has been widely accepted to improve the structural stability and electrochemical performance of layer transition metal oxides.

As discussed previously, the surface stability of Ni-rich cathode is a key issue for their electrochemical performance. The residual lithium oxide at the particle surface after annealing tends to absorb moisture and CO_2 in air during storage, leading to the formation of some unwanted products on the surface such as LiOH and Li_2CO_3. These products would react with electrolyte, forming surface interface. In addition, Ni^{4+} at the delithiated state would accelerate the decomposition of electrolyte, further resulting in the thickening of interfaces and sluggish Li^+ diffusion kinetics. Considering these problems, surface protection of Ni-rich cathode materials is highly desirable such as various surface coatings including metal oxide, phosphates, carbon, fluorides, artificial SEI, and conducting polymers [11].

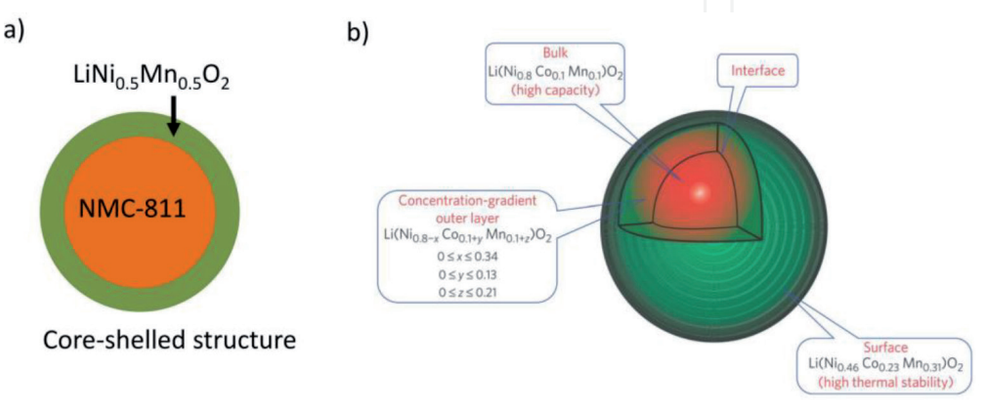


Figure 5.
(a) Core-shelled structure NMC: core: NMC-811 and shell: LiNi0.5Mn0.5O2; (b) concentration gradient-based NMC cathode.

DOI: http://dx.doi.org/10.5772/intechopen.84534

3. Spinel cathode

3.1 Spinel $LiMn_2O_4$

In contrast to layered $LiCoO_2$, spinel $LiMn_2O_4$ possesses more stable structure and higher voltage (4.0 V). As shown in **Figure 6**, $LiMn_2O_4$ has a cubic crystal structure with Li occupying the tetrahedral 8a sites and Mn occupying the octahedral 16d sites. The interstitial sites for Li, 16c, share faces with the occupied sites, forming a continuous three-dimensional diffusion network by the $[Mn_2O_4]$ framework. Thackeray et al. have demonstrated that lithium can be reversibly intercalated and deintercalated for the range of $0 < x < 2.2$ in $Li_xMn_2O_4$ in the cutoff range (2–4.5 V) with two plateaus at 4.0 and 3.0 V [15]. However, $LiMn_2O_4$ is usually cycled in the voltage range of 3.5–4.5 V because of the poor structural stability during cubic-tetragonal phase transition for $1 < x < 2$ in the cutoff window (2–4.5 V). Such cubic-tetragonal phase transition is driven by the Jahn-Teller distortion of MnO_6 octahedron as Mn^{4+} is reduced to Mn^{3+}, leading to a 6.5% increase of the unit cell volume. Thus, the specific capacity available for $LiMn_2O_4$ is theoretical 148 mAh g^{-1}. More importantly, $LiMn_2O_4$ just needs to use earth-abundant and low-cost Mn resources without using Ni and Co element, which is very beneficial for its large-scale application.

Although spinel $LiMn_2O_4$ shows attractable merits for LIBs, it also suffers from some drawbacks, such as Jahn-Teller distortion and Mn dissolution. To inhibit the Jahn-Teller distortion, doping with Li or multivalent cations (e.g., Al, Mg) has been widely used because partial replacement of Mn can reduce the Mn^{3+} concentration and increase the average valence of Mn, thus suppressing the onset of Jahn-Teller effect. Although metal-doped $LiMn_2O_4$ shows the enhanced electrochemical properties, it inevitably reduces the theoretical capacity owing to inactive element introduction. In this regard, a small amount of metal substitution is desirable. Another problem for spinel $LiMn_2O_4$ is the Mn dissolution owing to the disproportionation reaction of Mn^{3+} by forming Mn^{4+} and soluble Mn^{2+} catalyzed by acidic species in the electrolyte. Moreover, Mn^{2+} can react with $LiPF_6$ salt to produce more acidic by-products. To mitigate or address such problems, the surface modification strategy has been extensively employed.

3.2 High-voltage spinel $LiNi_{0.5}Mn_{1.5}O_4$

Besides 4 V-spinel, another Mn-based spinel $LiNi_{0.5}Mn_{1.5}O_4$ (LNMO) also shows considerable attention for LIBs in recent years. Owing to high working voltage (4.7 V vs. Li/Li^+), such spinel shows the highest specific energy (650 wh kg^{-1} at a material level) compared to other cathode materials (LCO, 540 Wh kg^{-1}; LFP,

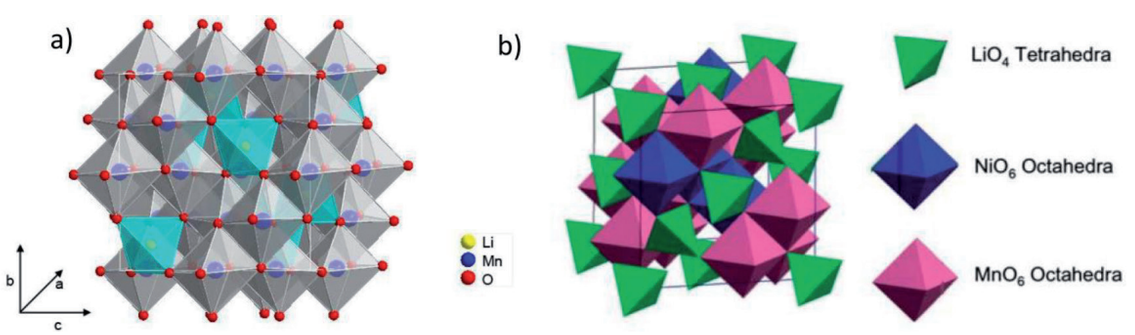


Figure 6.
Crystal structures of (a) spinel LiMn2O4 and (b) spinel LiNi0.5Mn1.5O4.

500 Wh kg^{-1}; LMO, 500 Wh kg^{-1}). The interstitial space in the spinel framework offers 3D Li^+ diffusion channels. Owing to its high working voltage, LNMO has become a very promising candidate for replacing spinel $LiMn_2O_4$ cathode. Moreover, relatively benign metal elements make such a material a top choice for next-generation high-power batteries. However, there are still some serious limitations to restrict its commercial applications. Ni is active with the two Ni^{2+}/Ni^{3+} and Ni^{3+}/Ni^{4+} couples at a 4.7 V, while Mn is inactive without capacity contribution. Although Ni^{2+}/Ni^{3+} and Ni^{3+}/Ni^{4+} electrochemical couples provide favorable high working voltage, they also bring some unwanted side reactions between active component and electrolyte, which gives rise to a considerable thickening of the protective solid-electrolyte interphase (SEI) layer passivating the material surface, thus leading to Li^+ ion diffusion obstacle.

High redox couple of Ni^{3+}/Ni^{4+} easily incurs the decomposition of conventional carbonate-based electrolyte. It is difficult for pure LNMO phase to be synthesized because of mixed ordered and disordered LNMO phase owing to oxygen deficiency caused by high-temperature annealing. In addition, the $Li_xNi_{1-x}O_2$ impurity probably forms as the second phase. Compared to ordered LNMO phase with $P4_332$ space group, disordered phase is relatively easily synthesized. The disordered spinel shows a better electrochemical performance than ordered spinel because the disordered one has an increased Li^+ ion diffusion coefficient. However, the presence of a small amount Mn^{3+} in the disorder phase will cause a non-negligible capacity fading during cycling, especially at elevated temperature. In this respect, introducing metal doping is an effective strategy to increase the average valence of Mn in the spinel. Mn^{3+} concentration in the spinel can be also decreased by reannealing treatment, which can also reduce oxygen defect and impurity amount, resulting in better electrochemical performance. In recent years, various strategies have been widely used to enhance electrochemical performance of LNMO, such as doping and surface coating. Metal doping can provide better chemical and structural stability and higher electrical conductivity. For example, Ti-doped LNMO improved the disordering of the transition metals and lowered the symmetry from simple cubic structure ($P4_332$) to face-centered spinel ($Fd3m$) [16]. Importantly, Ti-doped LNMO spinel shows higher working voltage, faster Li^+ ion diffusion, and better rate capability than undoped spinel. Fe doping in the high-voltage spinel can stabilize the solid during repeated cycling, leading to better cycling performance [17]. Thus, double doping by using Ti and Fe is an effective strategy to synergistically enhance the structural stability of LNMO. Additionally, other dopants including Cr, Ru, Zr, Al, and Mg can show better rate capability and cycling performance. Besides metal doping, anion dopant can also enhance electrochemical performance of high-voltage spinel. For example, the F-doped LNMO can restrict the formation of NiO impurity and change the lattice parameters and bonding energy [18], leading to fine structure and significantly enhanced cycling performance.

On the other hand, similar to layered NMC, the interface stability of LNMO between electrode and electrolyte is also a key for achieving long-term cycling performance. It has been demonstrated that better stability can be obtained by coating more stable surface layer, such as metal (Zn, Au, Ag), metal oxides (ZnO, SnO_2, ZrO_2), and metal phosphates (Li_3PO_4). For instance, ZnO-coated LNMO can effectively suppress Mn dissolution and increase the stability. More importantly, HF content in the electrolyte can be restricted because ZnO protection layer acts as a scavenger of fluoride anions from HF generated from the decomposition of $LiPF_6$ salt in the electrolyte by transforming HF to ZnF_2 [19, 20]. Li_3PO_4 protects the surface of LNMO and functions as a solid-electrolyte interface between active component and solid polymer electrolyte (SPE) to prevent the SPE degradation [21]. Such findings show that surface coating can not only enhance structural stability of LNMO but also restrict Mn dissolution, thus leading to improved cycling stability.

4. Polyanion-based cathode

4.1 Olive $LiFePO_4$

Polyanion cathode materials have received considerable attention in LIBs owing to their stable crystal structure and long-term cycling performance. Since John B. Goodenough proposed $LiFePO_4$ as cathode materials for LIBs in 1997, it has received much investigation including academic and industrial activities. As shown in **Figure 7**, $LiFePO_4$ possesses an olive structure with space group Pnma. The O atoms are located in a slightly distorted, hexagonally close-packed arrangement. The P atoms occupy tetrahedral sites, while Li and Fe atoms occupy octahedral 4c and 4a sites, respectively. The LiO_6 octahedra from edge-sharing chain along the b-axis. Each FeO_6 octahedron is linked with four FeO_6 octahedra by common corners in the b–c plane, forming zigzag planes. One FeO_6 octahedron has common edges with two LiO_6 octahedra. PO_4 groups share one edge with one FeO_6 octahedron and two edges with LiO_6 octahedra.

Compared to layered $LiCoO_2$, $LiFePO_4$ has excellent structural stability and thermal stability owing to the strong covalent P-O bonds in the $(PO_4)^{3-}$ polyanionic clusters. The host framework can make host stable enough upon repeating cycling without evident structural changes and temperature limitations and no loss of oxygen. These advantages offer safe enough application for LIBs. However, long-term air exposure at a moderate temperature will give rise to surface oxidation of $LiFePO_4$/C nanocomposites with the formation of a $LiFePO_4(OH)$ phase. Despite these drawbacks, the advantages of LFP including cycle stability, safety, environmental friendliness, and low cost make this material a very promising cathode candidate in LIBs. Currently, it has been successfully commercialized by many battery manufactures such as A123 and BYD.

Although $LiFePO_4$ possesses many merits, it still has some drawbacks such as low intrinsic electric conductivity (~ 10^{-9} S cm^{-1}) and low packing density. During past decades, much effort has been focused on addressing these problems by optimizing synthesis method, surface modification, reducing particle size, and metal doping [22]. Among them, surface modification has been widely accepted as an effective approach for enhancing the electronic conductivity of $LiFePO_4$. Carbon coating is the most popular surface modification strategy for $LiFePO_4$. It can not only improve the electric conductivity of active particle but also act as a reducing agent to prevent the formation

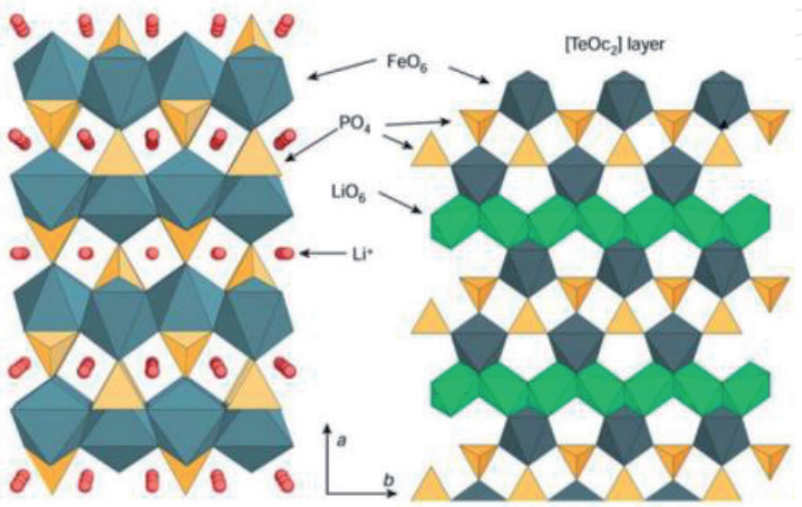


Figure 7.
The crystal structure of olivine LiFePO4 in projection along [001].

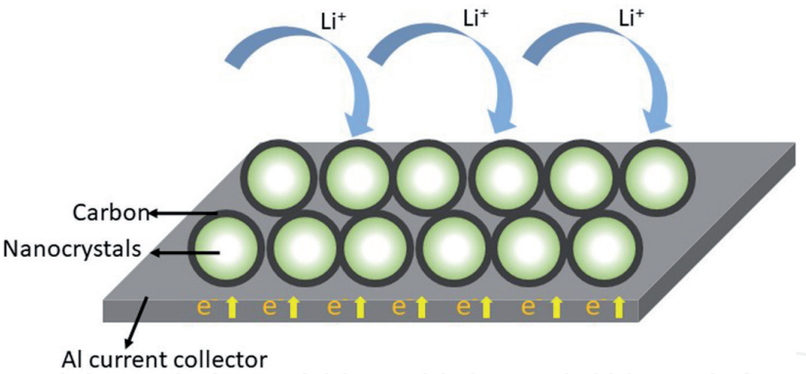


Figure 8.
Schematic diagram illustrating Li+ ion and electron transport pathways for active nanoparticle.

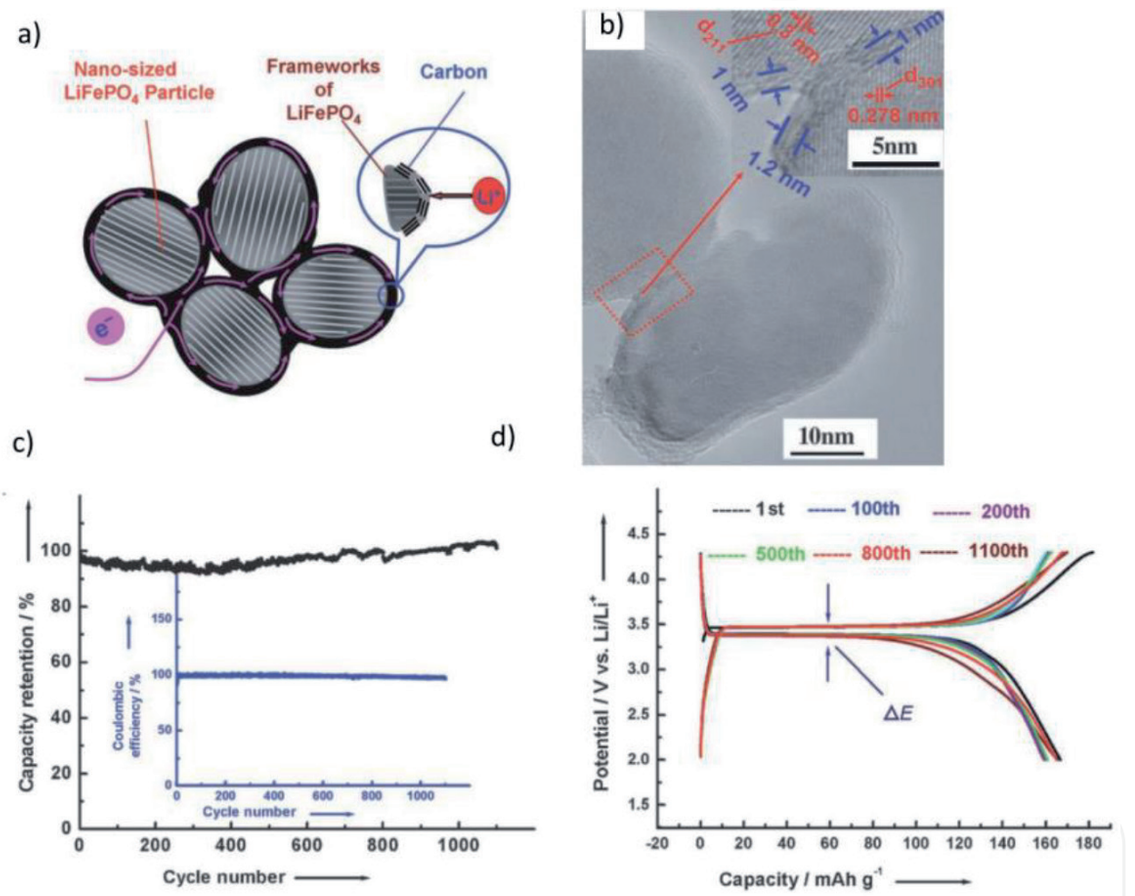


Figure 9.
(a) The ideal structure of carbon-coated LiFePO4 nanoparticles by a complete and uniform coating, (b) HRTEM image of carbon-coated LiFePO4 single nanoparticles, (c) cycling performance of carbon-coated LiFePO4 at a current density of 0.1 A g^{-1} between 2.0 and 4.3 V, and (d) charge/discharge profiles at different cycle numbers.

of Fe^{3+} impurity phase, as illustrated in **Figure 8**. In the meanwhile, the dense protection layer can effectively isolate the $LiFePO_4$ particle to inhibit the undesirable particle growth and self-aggregation. Nevertheless, a large amount of carbon reduces the volumetric energy density of the electrode. Various carbon sources have been used to generate carbon layer such as sucrose, starch, resorcinol-formaldehyde gel, sugar, carbon black, polypropylene, hydroxyethylcellulose, and so forth [22]. Therefore, carbon coating should be thin enough on the active particle surface. Wang et al. prepared uniform carbon-coated $LiFePO_4$ nanoparticle by an in situ polymerization restriction method for the synthesis of C/$LiFePO_4$ nanocomposite with a semi-graphitic carbon shell with a thickness of 1–2 nm [23], as shown in **Figure 9**. Charge/discharge tests

show that the so-formed nanocomposites exhibit superior rate capability and cycling stability (**Figure 9**). In addition to the effect of carbon content in the nanocomposite, the resultant carbon by different organic precursors shows different electronic conductivities, indicating that sp^2-coordinated carbon exhibits higher electronic conductivity than sp^3-coordinated or amorphous carbonaceous materials. Besides carbon coating, other surface modifications including metallic conducting layer and conducting polymer film are also investigated to enhance the electrochemical performance of $LiFePO_4$. Besides $LiFePO_4$, other polyanion-based cathode materials have also been developed such as $Li_3V_2(PO_4)_3$, $LiFeSO_4F$, $LiFeSiO_4$, and so on.

5. Li-free cathode

Besides the above Li-containing cathode, there are some Li-free cathode materials that have been studied for LIBs. The most common one is vanadium oxide. Owing to the multiple valence characteristic of vanadium (+2, +3, +4, +5), vanadium pentoxide (V_2O_5) possesses versatile redox-dependent properties and exhibits a great potential in the rechargeable batteries. V_2O_5 has a typical layered structure, which is very beneficial to Li^+-ion intercalation/de-intercalation. In recent years, V_2O_5 has been widely studied as cathode materials for LIBs. V_2O_5 is a typical intercalation compound with a layer structure with an orthorhombic structure belonging to P_mmn space group. **Figure 10** shows the crystal structure of orthorhombic V_2O_5, which consists of edge- and corner-sharing layered square pyramids, forming V_2O_5 nanosheets linked together by a weak V-O interaction orthogonal to the c-direction. In a single-layer slab, there are three crystallographically distinct oxygen centers (O1, O2, and O3). The single coordinated terminal/apical vanadyl oxygen atom, O(1), has a relatively short V-O bond length of ca. 1.54 Å; the bridging O2 oxygen connects with two adjacent V atoms by corner-sharing VO_5 square pyramids. The corresponding V-O bond length is ca. 1.77 Å. The O3 with triply coordinated chaining O atoms connects three V atoms by edge-sharing VO_5 square pyramids, and the three corresponding V-O bond length are 1.88, 1.88, and 2.02 Å. The orthorhombic V_2O_5 can be described as highly distorted VO_6 octahedral building blocks to form the layered anisotropic structure. The long sixth V-O bond underlines the structural anisotropy of such material and the ability to insert guest species in perovskite-like cavities. During lithium insertion into layered V_2O_5, it will induce the formation of vanadium bronzes as follows:

$$V_2O_5 + xLi^+ + xe^- = Li_xV_2O_5 \quad (1)$$

Besides crystallized V_2O_5, hydrated vanadium pentoxide ($V_2O_5\ nH_2O$) also shows promising lithium storage properties, such as $V_2O_5\ nH_2O$ xerogels, $V_2O_5\ nH_2O$ aerogels, and $V_2O_5\ nH_2O$ glasses [24]. These low crystalline or amorphous materials exhibit attractive merits owing to their unique nanostructures (high active surface

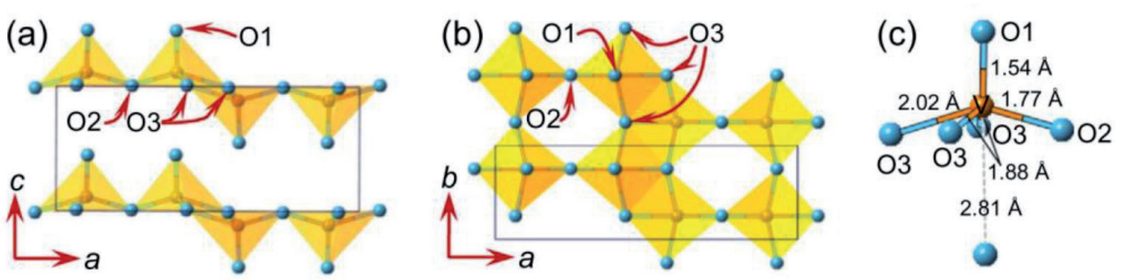


Figure 10.
Crystal structure of orthorhombic V2O5, view from (a) ac plane, (b) ab plane, and (c) the coordination environment around a single vanadium atom. The V and O atoms are represented in yellow and blue spheres.

area, small particle size, high diffusion coefficients, low-volume change upon repeated Li insertion/extraction processes). An effective approach to increase the intercalation capacity of V_2O_5 is to adjust the interlayer structure and the interaction forces between the adjacent layers. Usually, when the interlayer distance between V_2O_5 layered structure increases, the lithium insertion capacity will increase. However, owing to the absence of lithium in the V_2O_5, Li metal or Li-containing anode must be used for LIBs.

6. Thin-film battery applications of cathode materials

Among various battery chemistries, thin-film batteries are considered as the most competitive power sources owing to their high volumetric energy density, gravimetric specific energy, superior power capability, and good flexibility, as shown in **Figure 11**. Each cell is constructed by cathode, anode, and electrolyte, which is the same to conventional LIBs. To achieve high specific energy of thin-film battery, two requirements must be met by electrode materials: (i) high specific charge density (in Ah kg^{-1} and Ah L^{-1}) and (ii) high cell working voltage that requires high cathode redox potential and low anode redox potential. In addition, electrode reactions should be highly reversible on both cathode and anode for guaranteeing good cycling performance. Thus, developing advanced battery chemistry

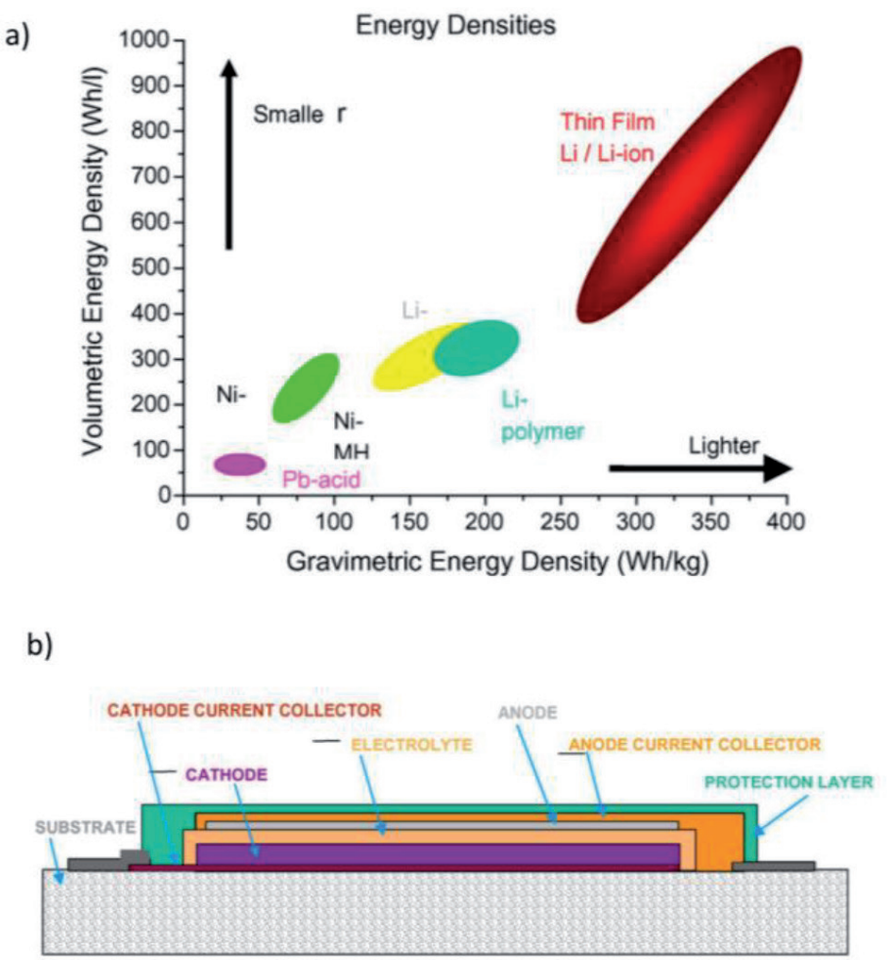


Figure 11.
(a) Comparison of the gravimetric and volumetric energy density of various chemical batteries including Pb-acid, Ni-MH, Li-ion batteries, and thin-film Li-ion batteries. (b) Cross-sectional schematic diagram of thin-film Li-ion battery.

is a key for high-performance thin-film batteries. This section only focuses on cathode materials for their thin-film microbattery application.

For practical cells, carbon-based anode and metal oxide cathode have been employed since they can offer maximum specific energy, sufficient power density, and long-term cycle life. Currently, several cathode materials ($LiCoO_2$, $LiNiO_2$, $LiMn_2O_4$, LNMO, and V_2O_5) are relatively popular. These electrodes are relatively stable in the air. In the case of V_2O_5, lithium metal laminate is attached to the carbon anode. After filling in the electrolyte, the metallic Li reacts with carbon and generates Li_xC_6, which is a lithium source in the cell.

$LiCoO_2$ is one of the most common used cathode materials for thin-film LIBs. Kuwata et al. prepared thin-film LIBs by using $LiCoO_2$, amorphous SnO, and amorphous Li_2O-V_2O_5-SiO_2 as cathode, anode, and solid electrolyte, respectively [25]. As illustrated in **Figure 12**, the battery has an area of about 0.23 cm^2, and the thickness is around 2 μm. All films were grown by PLD. The thin-film battery is fabricated on the quartz glass substrate, and metal Pt was deposited by PLD onto the substrate as a current collector. The solid electrolyte $Li_{3.4}V_{0.6}Si_{0.4}O_4$ was prepared by solid-state reaction from Li_2CO_3, SiO_2, and V_2O_5 and then was pressed into a disk with a diameter of 13 mm and annealed at 1100°C for the targets. The $LiCoO_2$ powder was pressed and sintered in air (900°C) as cathode, and the SnO powder was pressed into the disk without annealing. As displayed in **Figure 12**, the thicknesses of SnO, LVSO, and $LiCoO_2$ films are estimated to be 150, 1100, and 400 nm, respectively. The total thickness of the battery is around 2 μm. The interface between the $LiCoO_2$, SnO, and LVSO electrolyte remained smooth before and after cycling.

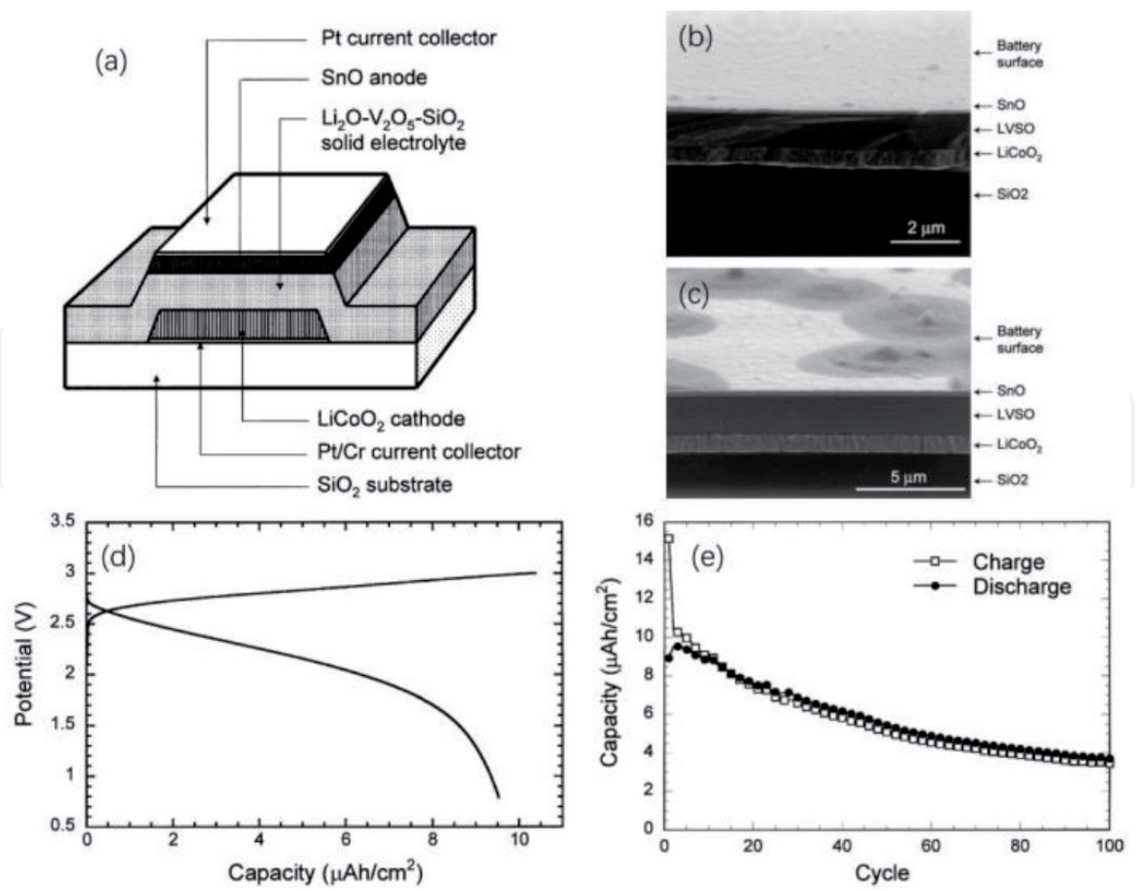


Figure 12.
(a) Schematic diagram (cross-sectional view) of thin-film LIBs, (b) SEM micrographs showing cross-sectional view before cycling, (c) after 100 cycles, (d) charge/discharge curves of the thin-film LIBs in the second cycle at a current of 44 mA/cm2, and (e) the specific capacity as a function of cycle number.

The thin-film battery was tested at a cutoff window of 3.0–0.7 V. As shown in **Figure 12**, the discharge capacity in the second cycle is about 9.5 mAh cm^{-2}, corresponding to 10–20% of $LiCoO_2$ utilization. The discharge potential gradually decreases in the range from 2.7 to 1.5 V owing to the amorphous nature of the SnO film. Such a thin-film battery shows a rapid capacity decay in the first cycle, which is probably attributed to the irreversible formation of Sn-Li alloy and amorphous Li_2O. Despite this, such battery was still cycled for 100 cycles with good Coulombic efficiency (**Figure 12**).

As discussed previously, various cathode materials ($LiCoO_2$, $LiMn_2O_4$, $LiFePO_4$, V_2O_5) have been studied for thin-film LIBs. However, they show limited specific energies. To further improve the energy density of the Li-ion thin-film microbattery, an effective solution is using high-potential cathode material. It is well known that LNMO is a very promising high-voltage cathode material owing to its high working potential at 4.7 V vs. Li/Li^+. Nowadays, LNMO thin films have been deposited by various techniques such as sol-gel, electrostatic spray deposition, pulsed laser deposition (PLD), and RF magnetron sputtering deposition. Letiche et al. prepared LNMO thin film on functional current collector by a radiofrequency magnetron sputtering method [26]. The authors first solved the technological issue owing to PtSi phase which originates from the interdiffusion between silicon wafer and Cr/Pt current collector to form PtSi phase under annealing treatment. By doping the Cr layer with a dense and pinhole-free Al_2O_3 thin film deposited by ALD acting as a barrier diffusion between the Si substrate and the LNMO layer, the synthesis process has been validated. In addition, the authors demonstrated that the deposition pressure plays a key role on the Ni-Mn cation ordering in spinel-like structure ($P4_332$ ordered vs. $Fd3m$ disordered spinel) and consequently on the electrochemical performance. It indicates that LNMO thin film deposited at 10^{-2} mbar and annealed at 700°C exhibits a normalized capacity of 65 µAh cm^{-2} $µm^{-1}$

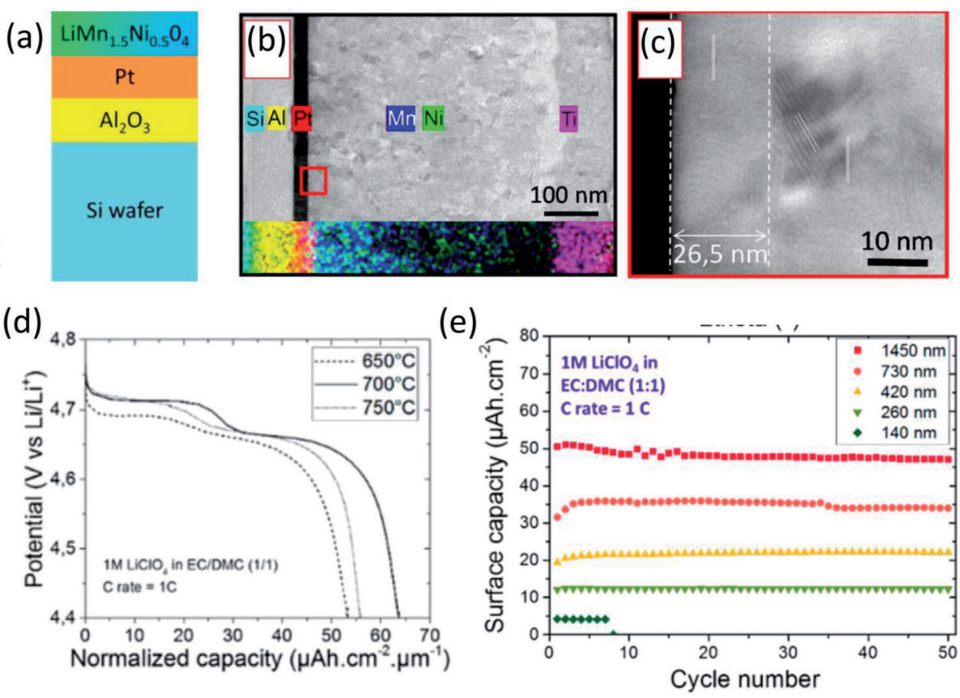


Figure 13.
(a) The as-prepared LNMO thin film, (b) TEM analysis of the cross section Si/Al2O3/Pt/LNMO/Ti/SiO2 prepared by focus ion beam technique, (c) HRTEM image of the LNMO layer with a focus close to the Pt current collector in order to check the Pt/LNMO interface, (d) discharge curve of LNMO thin film at different annealing temperatures, and (e) evolution of the surface capacity vs. cycle number as a function of the thin-film thickness.

with good capacity retention during cycling. The Coulombic efficiency is highly dependent on the film thickness of high-voltage thin-film electrodes.

As shown in **Figure 13**, the TEM image obtained by the focused ion beam (FIB) technique shows the different stacked layers on Si wafer where the thickness is close to 85 nm for Al_2O_3, 30 nm for Pt current collector, and 480 nm for LNMO thin-film electrode. Moreover, LNMO layer exhibits a polycrystalline nature with a different crystallized orientation (domains of ~ 20 nm), except for a thickness of 26.5 nm along the Pt layer where a (111) preferred orientation is seen, as displayed in **Figure 13**. The LNMO thin film annealed at 700°C delivers the best performance.

7. Conclusions

This chapter mainly discusses the development of currently the state-of-art cathode materials for LIBs and analyzes their potential applications in thin-film Li-ion microbatteries. For Li-containing cathode, layered structured $LiCoO_2$, NMC, and NCA, spinel $LiMn_2O_4$, and polyanion-based $LiFePO_4$ are currently the most popular for LIBs. Among them, $LiCoO_2$ is mainly used in the field of consumer electronics, while $LiMn_2O_4$, $LiFePO_4$, NMC, and NCA can be employed as power battery cathode materials for EVs. In particular, Ni-rich NCA and NMC-811 have been currently considered as the most attractive cathode candidate for long-range EVs due to their high specific energy compared to Ni-less NMC. In this respect, Ni-rich NMC cathode shows a sizable potential for high-energy thin-film LIBs in the future, but they are seldom investigated in thin-film Li-ion battery. Besides developing high-capacity cathode materials for realizing high-energy thin-film LIBs, exploiting high-potential cathode materials is also an effective strategy. Spinel LNMO is a very promising cathode candidate owing to its high redox potential (4.7 V vs. Li/Li^+), which has been widely investigated as cathode for thin-film LIBs. Additionally, Li-free cathode materials including V_2O_5, V_6O_{13}, MoS_2, TiS_2, and MnO_2 show attractive advantages for thin-film LIBs. Finally, the commercial success of thin-film Li-ion batteries will largely depend on the significant breakthrough of electrode materials including cathode, anode, and solid electrolyte in terms of energy density, weight, size, flexibility, and electrode/electrolyte interface.

Author details

Yuan-Li Ding
Hunan University, College of Materials Science and Engineering, Changsha, China

*Address all correspondence to: ylding@hnu.edu.cn

IntechOpen

© 2020 The Author(s). Licensee IntechOpen. Distributed under the terms of the Creative Commons Attribution - NonCommercial 4.0 License (https://creativecommons.org/licenses/by-nc/4.0/), which permits use, distribution and reproduction for non-commercial purposes, provided the original is properly cited. BY–NC

References

[1] Nishi Y. Lithium ion secondary batteries; past 10 years and the future. Journal of Power Sources. 2001;**100**(1-2):101-106

[2] Li H et al. Research on advanced materials for Li-ion batteries. Advanced Materials. 2009;**21**(45):4593-4607

[3] Liu C, Neale ZG, Cao G. Understanding electrochemical potentials of cathode materials in rechargeable batteries. Materials Today. 2016;**19**(2):109-123

[4] Goodenough JB, Park KS. The Li-ion rechargeable battery: A perspective. Journal of the American Chemical Society. 2013;**135**(4):1167-1176

[5] Chen Z, Dahn JR. Methods to obtain excellent capacity retention in $LiCoO_2$ cycled to 4.5 V. Electrochimica Acta. 2004;**49**(7):1079-1090

[6] Barker J, Koksbang R, Saidi MY. An electrochemical investigation into the lithium insertion properties of Li_xNiO_2 ($0 \leq \times \leq 1$). Solid State Ionics. 1996;**89**:25-35

[7] Liu W et al. Nickel-rich layered lithium transition-metal oxide for high-energy lithium-ion batteries. Angewandte Chemie. 2015;**54**(15):4440-4457

[8] Manthiram A. An outlook on Lithium ion battery technology. ACS Central Science. 2017;**3**(10):1063-1069

[9] Peralta D et al. Submicronic $LiNi_{1/3}Mn_{1/3}Co_{1/3}O_2$ synthesized by co-precipitation for lithium ion batteries—Tailoring a classic process for enhanced energy and power density. Journal of Power Sources. 2018;**396**:527-532

[10] Gruber PW et al. Global Lithium availability: A constraint for electric vehicles. Journal of Industrial Ecology. 2011;**15**(5):760-775

[11] Manthiram A, Song B, Li W. A perspective on nickel-rich layered oxide cathodes for lithium-ion batteries. Energy Storage Materials. 2017;**6**:125-139

[12] Noh H et al. Comparison of the structural and electrochemical properties of layered $Li[Ni_xCo_yMn_z]O_2$ (x = 1/3, 0.5, 0.6, 0.7, 0.8 and 0.85) cathode material for lithium-ion batteries. Journal of Power Sources. 2013;**233**:121-130

[13] Sun Y et al. Synthesis and characterization of $Li[(Ni_{0.8}Co_{0.1}Mn_{0.1})_{0.8}(Ni_{0.5}Mn_{0.5})_{0.2}]O_2$ with the microscale Core–Shell structure as the positive electrode material for Lithium batteries. Journal of the American Chemical Society. 2005;**127**(38):13411-13418

[14] Sun Y et al. High-energy cathode material for long-life and safe lithium batteries. Nature Materials. 2009;**8**(4):320-324

[15] Thackeray MM. Spinel electrodes for Lithium batteries. Journal of the American Ceramic Society. 2004;**82**(12):3347-3354

[16] Kim J-H et al. Effect of Ti substitution for Mn on the structure of $LiNi_{0.5}Mn_{1.5-x}Ti_xO_4$ and their electrochemical properties as Lithium insertion material. Journal of the Electrochemical Society. 2004;**151**(11):A1911-A1918

[17] Alcantara R et al. Synergistic effects of double substitution in $LiNi_{0.5-y}Fe_yMn_{1.5}O_4$ spinel as 5 V cathode materials. Journal of the Electrochemical Society. 2005;**152**(1):A13-A18

[18] Xu X et al. $LiNi_{0.5}Mn_{1.5}O_{3.975}F_{0.05}$ as novel 5 V cathode material. Journal of Power Sources. 2007;**174**(2):1113-1116

[19] Sun Y-K et al. Electrochemical performance of nano-sized ZnO-coated $LiNi_{0.5}Mn_{1.5}O_4$ spinel as 5 V materials at elevated temperatures. Electrochemistry Communications. 2002;**4**(4):344-348

[20] Sun Y-K, Yoon C, Oh I-H. Surface structural change of ZnO-coated $LiNi_{0.5}Mn_{1.5}O_4$ spinel as 5 V cathode materials at elevated temperatures. Electrochimica Acta. 2003;**48**(5):503-506

[21] Kobayashi Y et al. 5 V class all-solid-state composite lithium battery with Li_3PO_4 coated $LiNi_{0.5}Mn_{1.5}O_4$. Journal of the Electrochemical Society. 2003;**150**(12):A1577-A1582

[22] Wang Y, He P, Zhou H. Olivine $LiFePO_4$: Development and future. Energy & Environmental Science. 2011;**4**(3):805-817

[23] Wang Y et al. The design of a $LiFePO_4$/carbon nanocomposite with a Core–Shell structure and its synthesis by an in situ polymerization restriction method. Angewandte Chemie. 2008;**47**(39):7461-7465

[24] Wang Y et al. Nanostructured vanadium oxide electrodes for enhanced Lithium-ion intercalation. Advanced Functional Materials. 2006;**16**(9):1133-1144

[25] Kuwata N et al. Thin-film lithium-ion battery with amorphous solid electrolyte fabricated by pulsed laser deposition. Electrochemistry Communications. 2004;**6**(4):417-421

[26] Letiche M et al. Tuning the cation ordering with the deposition pressure in sputtered $LiMn_{1.5}Ni_{0.5}O_4$ thin film deposited on functional current collectors for Li-ion microbattery applications. Chemistry of Materials. 2017;**29**(14):6044-6057